all bond angles = 109.47. C_6H_5P: C-P = 1.83, C-C = 1.40, C-H = 1.08, all bond angles = 120.

Metal Fragments. For C_{4v} ML_5 and C_{2v} ML_3, all the valence angles at the metal are equal to 90°. This gives, for V(Cp)$(CO)_2$, ∠Cp(centroid)VC(O) = CpVP(PH_2) = 125.26°. For C_{2v} ML_4 and $C_{2v}ML_2$, the valence angle at the metal between equatorial ligands is 120°. Again CpMC(O) = 125.26°. For C_{3v} ML_3, all valence angles at the metal = 90°. Bond lengths (Å): W-H = 1.80, W-C(O) = 2.06, V-Cp(centroid) = 1.95, V-C(O) = 1.90, Ni-F = 1.99, Pt-Cl = 2.30, Cr-C(O) = 1.92, Fe-C(O) = 1.80, Mn-C(O) = 1.80, Mn-Cp = 1.80, Fe-Cp = 1.70, Fe-C_6H_6-(centroid) = 1.55, Co-Cp = 1.80, Ni-C(N) = 1.90, Ni-Cl = 2.32, (W)C-O = 1.15, (V)C-O = 1.15, (Cr)C-O = 1.17, (Fe)C-O = 1.15, (Mn)C-O = 1.15, Mn-H = 1.60, W-Cl = 2.30, Ni-C(O) = 1.83, (Ni)C-O = 1.15, (Ni)C-N = 1.15. In Cp and C_6H_6 bond distances (Å) are C-C = 1.42 and C-H = 1.08.

The metal-phosphinidene distance was fixed at 2.00 Å in all η^1 complexes. In the η^2 complex H_2PP-$PtCl_3^-$, the distance between the center of the P-P bond and the metal was fixed at 2.00 Å, corresponding to a Pt-P distance of 2.3 Å. The metal-nitrene distance was fixed at 1.80 Å. In the η^4 complexes the distance between the central phosphorus and the metal was fixed at 2.00 Å. In the μ_2 complexes, the metal-phosphinidene distance was fixed at 2.20 Å and the MPM angle was fixed at 138°.

Contribution from the Departments of Chemistry, Cornell University, Ithaca, New York 14853, and University of St. Andrews, St. Andrews, Fife K716 9ST, Scotland, U.K.

Bonding in Nitrosylated Iron-Sulfur Clusters

SHEN-SHU SUNG,† CHRISTOPHER GLIDEWELL,*‡ ANTHONY R. BUTLER,‡ and ROALD HOFFMANN*†

Received August 6, 1984

The electronic structure of several binuclear and tetranuclear Fe clusters with bridging S or SH units and terminal nitrosyl ligands is analyzed. The computations point to the antibonding nature of the lowest unoccupied orbitals of these molecules, indicative of potential disruption of the clusters on reduction.

The known nitrosylated iron-sulfur cluster molecules and ions[1-4] $Fe_4S_4(NO)_4$, $[Fe_4S_3(NO)_7]^-$, $[Fe_2S_2(NO)_4]^{2-}$, and $Fe_2(SR)_2(NO)_4$ are closely related to each other chemically, as shown by the transformations[1,3,5,6]

$$Fe_2(SR)_2(NO)_4 \xleftarrow{RX} [Fe_2S_2(NO)_4]^{2-} \underset{OH^-}{\overset{H^+}{\rightleftharpoons}}$$

$$[Fe_4S_3(NO)_7]^- \underset{Na/Hg}{\overset{S_8}{\rightleftharpoons}} Fe_4S_4(NO)_4$$

Although these species are all diamagnetic in the solid state and in weak-donor solvents, in powerful donor solvents they all readily yield paramagnetic species containing a single iron atom.[7] The reduction of $Fe_4S_4(NO)_4$ yields, initially, the anion $[Fe_4S_4(NO)_4]^-$, which is subsequently converted into $[Fe_4S_3(NO)_7]^-$ along with uncharacterized byproducts. This reductive transformation is effected[2] in a solvent, THF/acetone, in which dissociation to mononuclear intermediates may occur, and it seems at least possible that both the conversion of $Fe_4S_4(NO)_4$ to $[Fe_4S_3(NO)_7]^-$ and the reverse of this may occur via a mechanism of extensive fragmentation and reassembly. The observation that $Fe_4S_4(NO)_4$ and $[Fe_4S_3(NO)_7]^-$ can both be synthesized by spontaneous self-assembly from mononuclear starting materials lends plausibility to this suggestion. Fragmentation must obviously occur in the conversion, in alkali, of $[Fe_4S_3(NO)_7]^-$ into $[Fe_2S_2(NO)_4]^{2-}$,[3] and in fact dilute aqueous alkaline solutions of $[Fe_4S_3(NO)_7]^-$ exhibit[7] ESR spectra characteristic of mononuclear iron-nitrosyl species; similarly oxidative transformation of $[Fe_4S_3(NO)_7]^-$ to $Fe_2I_2(NO)_4$ must involve some form of fragmentation and reformation accompanying the redistribution of the nitrosyl groups.

As part of a broader study[7-12] of nitrosylated iron-sulfur clusters, occasioned partly by their suspected carcinogenicity,[13] we have carried out extended Hückel calculations on several of these systems, in order to shed some light on their transformations, in particular the propensity of the tetranuclear species to undergo significant molecular reorganization as the result of both electron addition and electron removal.

Idealized geometries of C_{3v}, T_d, D_{2h}, and C_{2h} symmetry were employed for $[Fe_4S_3(NO)_7]^-$, $Fe_4S_4(NO)_4$, $[Fe_2S_2(NO)_4]^{2-}$, and the prototype neutral two-iron system $Fe_2(SH)_2(NO)_4$, with dimensions derived from the experimentally determined structures.[1,2,4] I-III are representations of the structures of $[Fe_4S_3$-

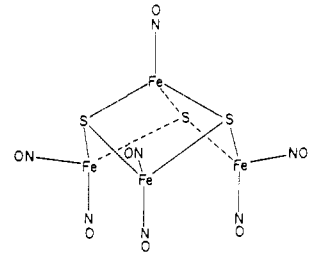

I

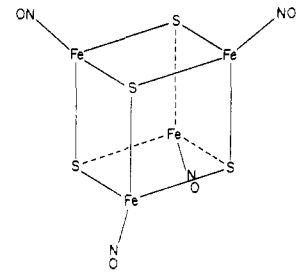

II

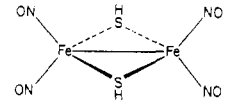

III

† Cornell University.
‡ University of St. Andrews.

(1) Chu, C. T.-W.; Lo, F. Y.-K.; Dahl, L. F. *J. Am. Chem. Soc.* **1982**, *104*, 3409.
(2) Chu, C. T.-W.; Dahl, L. F. *Inorg. Chem.* **1977**, *16*, 3245.
(3) Roussin, F. Z. *Ann. Chim. Phys.* **1858**, *52*, 285.
(4) Thomas, J. T.; Robertson, J. H.; Cox, E. G. *Acta Crystallogr.* **1958**, *11*, 599.
(5) Glidewell, C.; McGinnis, J. *Inorg. Chim. Acta* **1982**, *64*, L171.
(6) Beck, W.; Grenz, R.; Götz, F.; Vilsmaier, E. *Chem. Ber.* **1981**, *114*, 3184.
(7) Butler, A. R.; Glidewell, C.; Hyde, A. R.; Walton, J. C. *Polyhedron*, in press.
(8) Butler, A. R.; Glidewell, C.; Hyde, A. R.; McGinnis, J.; Seymour, J. E. *Polyhedron* **1983**, *2*, 1045.
(9) Butler, A. R.; Glidewell, C.; Hyde, A. R.; McGinnis, J. *Polyhedron* **1983**, *2*, 1399.
(10) Butler, A. R.; Glidewell, C.; Hyde, A. R.; Walton, J. C. *Polyhedron* **1985**, *4*, 303.
(11) Glidewell, C.; Hyde, A. R. *Polyhedron*, in press.
(12) Butler, A. R.; Glidewell, C.; Hyde, A. R.; McGinnis, J. *Inorg. Chem.* **1985**, *24*, 2931.
(13) Wang, G.-H.; Zhang, W.-X.; Chai, W.-G. *Adv. Mass Spectrom.* **1982**, *8B*, 1369.

0020-1669/85/1324-3856$01.50/0

Table I. Calculated Energy Levels (eV) and Their Bonding Character

$[Fe_4S_3(NO)_7]^-$, C_{3v}				$Fe_4S_4(NO)_4$, T_d				$Fe_2(SH)_2(NO)_4$, C_{2h}			
LUMO:	−10.07	E	Fe_4 *ab*	LUMO:	10.14	T_1	Fe_4 *ab*	LUMO:	−9.87	B_g	Fe_2 *ab*
HOMO:	−11.36	A_1	Fe_4 *b*	HOMO:	−11.41	T_2	Fe_4 *nb*	HOMO:	−11.98	B_u	Fe_2 *b*
	−11.80	E	Fe_4 *ab*		−12.03	A_1	Fe_4 *b*		−12.02	A_g	Fe_2 *b*
	−12.01	A_1	Fe_4 *ab*		−12.37	T_2	Fe_4 *b*		−12.02	B_g	Fe_2 *ab*
	−12.13	E	Fe_4 *b*		−12.50	E	Fe_4 *nb*		−12.37	B_u	Fe_2 *b*
	−12.52	E	Fe_4 *b*		−12.83	T_1	Fe_4 *nb*		−12.70	A_g	Fe_2 *b*
	−12.52	A_2	Fe_4 *ab*		−13.28	E	Fe_4 *b*		−12.74	B_g	Fe_2 *ab*
	−12.91	E	Fe_4 *nb*						−13.16	A_u	Fe_2 *ab*
	−13.13	A_1	Fe_4 *b*						−13.31	A_u	Fe_2 *ab*
	−13.15	A_2	Fe_4 *b*						−13.34	A_g	Fe_2 *b*
	−13.17	E	Fe_4 *nb*								
	−13.40	E	Fe_4 *nb*								
	−14.25	E	S(3p)-Fe, *b*		−14.31	E	S(3p)-Fe, *b*		−14.04	B_g	S(3p)-Fe, *b*
	−14.52	A_1			−14.33	A_1			−14.24	B_u	
	−14.56	E			−14.46	T_1			−14.39	A_g	
	−14.62	A_2			−14.59	T_2			−14.89	A_u	
	−15.09	E			−15.30	T_2					
	−15.13	A_1									
	−15.39	E	basal NO(5σ)		−15.54	T_2	NO(5σ)		−15.38	B_g	NO(5σ)
	−15.42	A_1			−15.61	A_1			−15.39	B_u	
	−15.54	A_1	apical						−15.48	A_g	
	−15.55	A_1	basal						−15.58	A_u	
	−15.65	E									
	−15.99	E	basal NO(π)		−16.12	T_1	NO(π)		−15.88	B_u	NO(π)
	−16.02	A_1			−16.13	E			−15.99	B_g	
	−16.05	A_2			−16.17	T_2			−16.02	A_g	
	−16.07	E							−16.04	B_g	
	−16.10	E	apical						−16.05	B_u	
	−16.14	A_2	basal						−16.11	A_u	
	−16.17	E							−16.14	B_u	S-H
	−16.20	E							−16.16	Au	NO(π)
	−16.24	A_1							−16.18	A_g	
	−20.82	E	S(3s)		−20.84	T_2	S(3s)		−16.40	Ag	S-H
	−21.35	A_1			−21.70	A_1			−21.75	B_u	S(3s)
									−21.89	A_g	
	−23.08	E	basal NO(4σ)		−23.36	T_2	NO(4σ)		−23.10	B_u	NO(4σ)
	−23.10	A_1			−23.59	A_1			−23.11	B_g	
	−23.48	A_1	apical						−23.68	A_u	
	−23.78	E	basal						−23.86	A_g	
	−23.95	A_1									
	−35.74	E	basal NO(3σ)		−35.86	A_1	NO(3σ)		−35.75	B_u	NO(3σ)
	−35.75	A_1	(eq)		−35.87	T_2			−35.75	B_g	
	−35.77	A_1	apical						−35.80	A_g	
	−35.80	E	basal						−35.80	A_u	
	−35.82	A_1	(ax)								

$(NO)_7]^-$, $Fe_4S_4(NO)_4$, and $Fe_2(SH)_2(NO)_4$. The $[Fe_2S_2(NO)_4]^{2-}$ structure is similar to III, except for the two H atoms of the thiolate groups.

All FeNO angles were additionally constrained to 180.0°, whereas experimentally the FeNO fragments are found to be bent in the solid state by up to 15°, in the case of the basal nitrosyl groups in $[Fe_4S_3(NO)_7]^-$: however, all the nitrosyl groups in these species are found in solution (which probably provides a closer approximation to isolated molecules than the crystalline phase) to be linear, according to the criterion of ^{15}N chemical shift.[14] Further details of the calculations are in the Appendix.

The calculated values of the binding energies of the occupied molecular orbitals of the valence shells, together with the LUMO in each case, are given for $[Fe_4S_3(NO)_7]^-$, $Fe_4S_4(NO)_4$, and $Fe_2(SH)_2(NO)_4$ in Table I. The occupied molecular orbitals and the LUMO of $[Fe_2S_2(NO)_4]^{2-}$ are very similar to those of $Fe_2(SH)_2(NO)_4$, except for the S–H bonding orbitals, which are replaced by the S 3p lone pairs. Also given in this table are the symmetry classes of the orbitals, within the point groups C_{3v}, T_d, and C_{2h}, respectively, and approximate descriptions of the principal components of the molecular orbitals. We use the symbols b for bonding, nb for nonbonding, and ab for antibonding. Although, in general, most of the molecular orbitals contain contributions from most of the component atomic orbitals, it is possible to ascertain by inspection of the eigenvectors the principal contributors in each case and to arrive at the approximate descriptions provided in Table I.

Low-Lying Orbitals

The general pattern of the binding energies is closely similar in all three species. At around −35.8 eV there is a set of MO's, corresponding in number in each molecule or ion to the number of nitrosyl groups, with a similar number of MO's at around −23.5 eV: these can be assigned to 3σ and 4σ of the nitrosyl groups, which are at energies −35.8 and −22.7 eV in the isolated nitrosyl fragment, respectively. The 3σ orbital has a larger component of oxygen 2s and 4σ that of a nitrogen 2s orbital. Similarly the sulfur 3s levels occur near −21.0 eV. At around −16 eV there is a substantial set of MO's, in each molecule or ion double the number of nitrosyl groups, which are made up principally of the π components of the nitrogen–oxygen bonds. In addition, the dinuclear $Fe_2(SH)_2(NO)_4$ contains two extra levels in this region, at −16.14 eV (B_u) and −16.40 eV (A_g), assignable to the sulfur–hydrogen bonding levels. The nitrosyl 5σ orbitals, whose larger component is oxygen 2p, lie at about −15.5 eV.

Sulfur–Iron Bonding

The bonding levels for the iron–sulfur bonds (three per sulfur in both $[Fe_4S_3(NO)_7]^-$ and $Fe_4S_4(NO)_4$, where each sulfur is bound only to three irons, but only two per sulfur in $Fe_2(SH)_2(NO)_4$, where each sulfur is bound to the iron atoms and one hydrogen) are in the range −14.0 to −15.3 eV. It is clear that, for each of these systems, although the bonding is to a large extent delocalized, the bonding involving the sulfurs can very readily be

(14) Bell, L. K.; Mingos, D. M. P.; Tew, D. G.; Larkworthy, L. F.; Sandell, B.; Povey, D. C.; Mason, J. *J. Chem. Soc., Chem. Commun.* **1983**, 125.

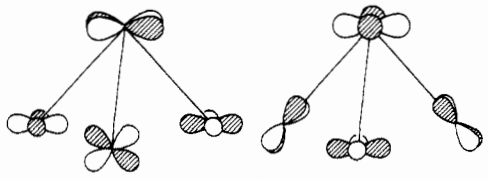

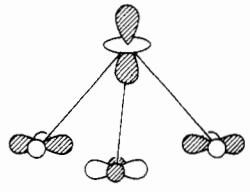

Figure 1. Frontier orbitals of $[Fe_4S_3(NO)_7]^-$. Only the main components, which are on the Fe atoms, are shown.

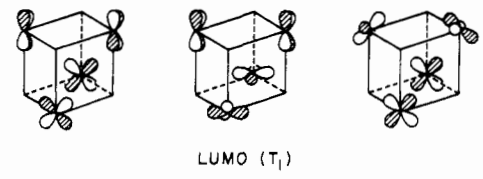

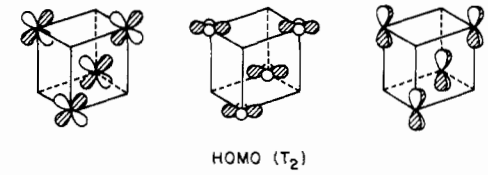

Figure 2. Frontier orbitals of $Fe_4S_4(NO)_4$. Only the main components, which are on the Fe atoms, are shown.

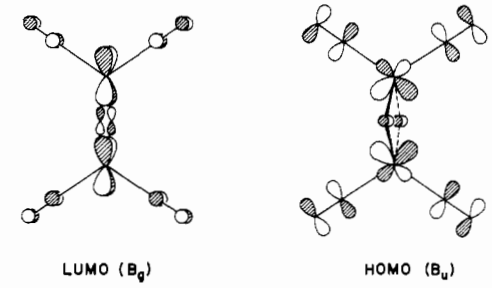

Figure 3. Frontier orbitals of $Fe_2(SH)_2(NO)_4$. $[Fe_2S_2(NO)_4]^{2-}$ has frontier orbitals very similar to these.

regarded in terms of electron pair bonds, involving sulfur 3p orbitals only, with the electron pairs occupying sulfur 3s orbitals behaving effectively as nonbonding (lone) pairs. In $[Fe_4S_3(NO)_7]^-$ there are, in the commonest representation of the structure (I), 9 electron-pair bonds involving sulfur, whereas in $Fe_4S_4(NO)_4$ (II) there are 12 such bonds: entirely in accord with these formulations, we calculate that there are exactly 9 occupied orbitals ($2A_1 + A_2 + 3E$) that are principally iron–sulfur bonding orbitals in $[Fe_4S_3(NO)_7]^-$ and exactly 12 such orbitals ($A_1 + E + T_1 + 2T_2$) in $Fe_4S_4(NO)_4$. In all of these orbitals the sulfur contribution is predominantly from 3p rather than 3s. In an entirely similar way, there are just four occupied bonding iron–sulfur orbitals in $Fe_2(SH)_2(NO)_4$ ($A_g + A_u + B_g + B_u$), consistent with the representation III containing four electron-pair iron–sulfur bonds.

Iron–Iron Bonding

The least tightly bound occupied orbitals, for each of these species, are those predominantly associated with the iron–iron interactions. In the anion $[Fe_4S_3(NO)_7]^-$ there are 17 occupied levels associated with the bonding of the Fe_4 cluster consistent with the usual assignment of formal oxidation states (reckoning the nitrosyl ligand as NO^+ and the μ_3-sulfur ligand as S^{2-}) as Fe^+ (d^7) for the apical iron and Fe^- (d^9) for the three basal irons. Of these 17 orbitals, seven ($2A_1 + A_2 + 2E$) may be described as bonding, six (3E) as nonbonding, and four ($A_1 + A_2 + E$) as antibonding with respect to the Fe_4 cage (see Table I), giving a net stabilization due to just six electrons in orbitals of symmetry ($A_1 + E$): in terms of localized bonding, this may be regarded as equivalent to one electron-pair bond between the apical iron and each basal iron. In particular it should be noted that while the HOMO is bonding with respect to the Fe_4 cluster, the LUMO is antibonding, as shown in Figure 1, so that either addition or removal of an electron is predicted to weaken the overall cage bonding. The overlap population between the apical iron and one basal iron is 0.138 in $[Fe_4S_3(NO)_7]^-$ and reduced to 0.118 by either removing or adding a pair of electrons from the HOMO or to the LUMO. The Fe–Fe bond weakening upon reduction is consistent with its ESR spectra[7] characteristic of mononuclear iron–nitrosyl species and the fragmentation in the conversion to $[Fe_2S_2(NO)_4]^{2-}$. Also the calculation results suggest the conversion to $Fe_4S_4(NO)_4$ via a mechanism of extensive fragmentation and reassembly.

The cubane-like cluster $Fe_4S_4(NO)_4$ contains 14 occupied levels associated with the Fe_4 cage bonding: this is again consistent with the assignment (on the same basis as before) of the formal oxidation state of +1 to the irons. There are eight essentially nonbonding Fe_4 orbitals ($E + T_1 + T_2$) and six bonding orbitals ($A_1 + E + T_2$) (see Table I), consistent with the qualitative suggestions of Chu and Dahl.[2] The 12 net bonding electrons may alternatively be regarded as forming an electron-pair bond along each of the 6 edges of the Fe_4 tetrahedron. Actually, the picture is somewhat complicated by interaction between bonding and nonbonding orbitals of the same symmetry. Thus the HOMO is not an Fe–Fe bonding orbital, but is nonbonding. The LUMO is antibonding with respect to the Fe_4 tetrahedral frame, as shown in Figure 2. Addition of electrons will weaken the cluster bonding; indeed, filling one of the pair of degenerate LUMO's will decrease the Fe–Fe overlap population 27% from its initial value of 0.121. But removal of electrons should not affect bond strengths.

Both $[Fe_4S_3(NO)_7]^-$ and $Fe_4S_4(NO)_4$ are calculated here to have degenerate LUMO's of E and T_1 symmetry, respectively. Consequently, electron addition will in each case give a Jahn–Teller-sensitive ion. In $[Fe_4S_3(NO)_7]^{2-}$, the system must distort along an E vibrational mode to give a product of C_s symmetry, whereas $[Fe_4S_4(NO)_4]^-$ could distort either along an E mode to a D_{2d} product or along a T_2 mode to a C_{3v} product. In fact $[Fe_4S_4(NO)_4]^-$ as its $[K(2,2,2\text{-crypt})]^+$ salt has rather exact D_{2d} symmetry: the dianion $[Fe_4S_3(NO)_7]^{2-}$ does not appear to have been identified, but the selenium analogue $[Fe_4Se_3(NO)_7]^{2-}$ as its $[Ba(2,2,2\text{-crypt})]^{2+}$ salt has[15] C_s symmetry, exactly in accord with the predictions based upon the calculated electronic structure for $[Fe_4S_3(NO)_7]^-$.

$[Fe_2S_2(NO)_4]^{2-}$ has an electronic structure very similar to that of $Fe_2(SH)_2(NO)_4$. The difference is that each sulfur atom in $[Fe_2S_2(NO)_4]^{2-}$ has a 3p lone pair at ~−14 eV with minor mixing of Fe orbitals, instead of S–H bonding as in $Fe_2(SH)_2(NO)_4$. In both these complexes, the iron atoms may be regarded as Fe^- (d^9): in accord with this formulation, there are nine occupied molecular orbitals that are primarily concentrated on the iron atoms. Of these, five (C_{2h}, $3A_g + 2B_u$; D_{2h}, $2A_g + B_{1g} + B_{2u} + B_{3u}$) are bonding, and four (C_{2h}, $2A_u + 2B_g$; D_{2h}, $A_u + B_{2g} + B_{3g} + B_{1u}$) are antibonding with respect to the iron–iron interaction, indicative of a net total of two bonding electrons (cf. III). Just as in the tetrairon complexes $[Fe_4S_3(NO)_7]$, the HOMO is bonding and the LUMO is antibonding between the two irons, as shown in

(15) Nelson, L. L. Ph.D. Thesis, University of Wisconsin—Madison, 1981.

Table II. Parameters Used in Extended Hückel Calculations

orbital		H_{ii}, eV	ζ_1	ζ_2	C_1[a]	C_2[a]
H	1s	−13.6	1.300			
N	2s	−26.0	1.950			
	2p	−13.4	1.950			
O	2s	−32.3	2.275			
	2p	−14.8	2.275			
S	3s	−20.0	1.817			
	3p	−13.3	1.817			
Fe	3d	−12.60	5.350	1.800	0.5366	0.6678
	4s	−9.10	1.900			
	4p	−5.32	1.900			

[a] These are the coefficients in the double-ζ expansion.

Figure 3. By removal of a pair of electrons from the HOMO of $Fe_2(SH)_2(NO)_4$, the Fe–Fe overlap population changes from 0.147 to 0.113, and by addition of a pair of electrons to its LUMO, the overlap population changes to 0.109. The Fe–Fe bond weakening upon reduction is consistent with the presence of paramagnetic species containing a single iron atom in powerful donor solvents.[7] Again, the Fe–N overlap population changes very little as we change electron occupation by 2.

The occupied iron–iron orbitals, together with the LUMO, in $Fe_2(SH)_2(NO)_4$ span the symmetry classes $3A_g + 2A_u + 3B_g + 2B_u$; on the other hand, the two sets of five 3d orbitals transform, in C_{2h}, as $3A_g + 3A_u + 2B_g + 2B_u$. Unlike the case for the tetranuclear complexes $[Fe_4S_3(NO)_7]^-$ and $Fe_4S_4(NO)_4$, the symmetry classes of the occupied orbitals cannot be classified in terms of those of the metal 3d orbitals: there is extensive p, d mixing in $Fe_2(SH)_2(NO)_4$, and this in part accounts for the anomaly. The presence of the two S substituents, in lowering of the molecular symmetry from D_{2h} to C_{2h}, removes the symmetry separation of π from δ Fe–Fe orbitals in C_{2h} and no symmetry factorization of the Fe–Fe orbitals is possible, while in D_{2h} the π orbitals (B_{2g}, B_{2u}, B_{3g}, B_{3u}) do not interact with either σ (A_g, B_{1u}) or δ (B_{1g}, A_u).

N–Fe Bonding

The bonding between the iron centers in these complexes and nitrosyl is similar to the well-known transition-metal–carbonyl interaction; that is, it is characterized by ligand 5σ to metal donation and metal to ligand π^* back-donation. But, unlike CO, whose 5σ orbital has a larger component on the carbon atom, the NO 5σ orbital is more concentrated on the oxygen. The s–p hybridization still gives 5σ good lone-pair character at N, but its donating capability in NO is not as good as in CO. This shows up in the electronic structure of the complexes. For example, the four orbitals at −15.39 to −15.58 eV in $Fe(SH)_2(NO)_4$ are mainly oxygen 2p lone pairs, with a small component on nitrogen and iron atoms. The strong iron to NO π^* back-donation manifests itself in several orbitals which are predominantly associated with the Fe–Fe interactions, rather than emerging in four or eight particular molecular orbitals. We can see this from Figure 3. This is why the overlap population between N and Fe atoms changes little on removing or adding a pair of electrons from its HOMO or to its LUMO.

Comparison with Other Iron–Sulfur Clusters

A number of previous calculations have been made,[16–20] using different approximations, for the natural-type iron–sulfur clusters $[Fe_2S_2(SR)_4]^{2-,3-}$ and $[Fe_4S_4(SR)_4]^{-,2-,3-}$ generally for the case of R = H. There appears to be no general agreement upon which theoretical model may prove to provide the best overall description of the spectroscopic and magnetic properties of such clusters.

Thus for $[Fe_2S_2(SH)_4]^{2-,3-}$, Xα-VB[18] and Xα-MO[16] calculations disagree on the nature of the highest occupied molecular orbitals. Arguments have been presented[20] that, for $[Fe_4S_4(SH)_4]^{2-}$, UHF wave functions must be used in Xα-MO calculations, rather than RHF functions, in order to accommodate the spin coupling between the several iron centers.

While for clusters of types $[Fe_2S_2(SR)_4]^{2-,3-}$ and $[Fe_4S_4(SR)_4]^{-,2-,3-}$ the magnetochemistry and EPR spectra have been studied in detail, thus providing experimental data that give searching tests of any theoretical model, at the present time no such data are available for any of the known nitrosylated iron–sulfur clusters. It is possible that when further physical data are available for such clusters, models more sophisticated than that employed here will be required to give even a qualitative interpretation.

Concluding Remarks

The antibonding nature of the LUMO of the nitrosylated iron–sulfur clusters discussed above is in good agreement with the fact that in powerful donor solvents they all readily yield species containing a single iron atom. Also, it points out the possibility that the interconversion of $Fe_4S_4(NO)_4$ and $[Fe_4S_3(NO)_7]^-$ may occur via a mechanism of extensive fragmentation and reassembly, like the conversion of $[Fe_4S_3(NO)_7]^-$ to $[Fe_2S_2(NO)_4]^{2-}$.

Acknowledgment. We are grateful to the National Science Foundation for its support of this research through Grant CHE 7828048 and to the Cancer Research Campaign (U.K.).

Appendix

The orbital exponents and H_{ii}'s for the extended Hückel calculations[21] were obtained from earlier work[22] and are listed in Table II.

Registry No. $[Fe_4S_3(NO)_7]^-$, 12518-87-5; $Fe_4S_4(NO)_4$, 53276-80-5; $[Fe_2S_2(NO)_4]^{2-}$, 97773-62-1; $Fe_2(SH)_2(NO)_4$, 97773-65-4.

(16) Norman, J. G., Jr.; Kalbacher, B. J.; Jackels, S. C. *J. Chem. Soc., Chem. Commun.* **1978**, 1027.
(17) Geurts, P. J. M.; Gosselink, J. W.; Van der Avoird, A.; Baerends, E. J.; Snijders, J. G. *Chem. Phys.* **1980**, *46*, 133.
(18) Norman, J. G., Jr.; Ryan, P. B.; Noodleman, L. *J. Am. Chem. Soc.* **1980**, *102*, 4279.
(19) Thomson, A. J. *J. Chem. Soc., Dalton Trans.* **1981**, 1180.
(20) Aizman, A.; Case, D. A. *J. Am. Chem. Soc.* **1982**, *104*, 3269.
(21) (a) Hoffmann, R. *J. Chem. Phys.* **1963**, *39*, 1397. (b) Hoffmann, R.; Lipscomb, W. N. *Ibid.* **1962**, *36*, 2179, 3489; **1962**, *37*, 2872.
(22) (a) Summerville, R. H.; Hoffmann, R. *J. Am. Chem. Soc.* **1976**, *98*, 7240. (b) Albright, T. A.; Hofmann, P.; Hoffmann, R. *Ibid.* **1977**, *99*, 7546.